Sept4/ARTS is required for stem cell apoptosis and tumor suppression

María García-Fernández,[1] Holger Kissel,[1] Samara Brown,[1] Travis Gorenc,[1] Andrew J. Schile,[1] Shahin Rafii,[2] Sarit Larisch,[3] and Hermann Steller[1,4]

[1]Laboratory of Apoptosis and Cancer Biology, Howard Hughes Medical Institute, The Rockefeller University, New York, New York 10065, USA; [2]Howard Hughes Medical Institute, Weill Medical College of Cornell University, New York, New York 10021, USA; [3]Cell Death Research Laboratory, Department of Biology, University of Haifa, Haifa 31905, Israel

Inhibitor of Apoptosis Proteins (IAPs) are frequently overexpressed in tumors and have become promising targets for developing anti-cancer drugs. IAPs can be inhibited by natural antagonists, but a physiological requirement of mammalian IAP antagonists remains to be established. Here we show that deletion of the mouse *Sept4* gene, which encodes the IAP antagonist ARTS, promotes tumor development. *Sept4*-null mice have increased numbers of hematopoietic stem and progenitor cells, elevated XIAP protein, increased resistance to cell death, and accelerated tumor development in an Eμ-*Myc* background. These phenotypes are partially suppressed by inactivation of XIAP. Our results suggest that apoptosis plays an important role as a frontline defense against cancer by restricting the number of normal stem cells.

[*Keywords*: Apoptosis; cancer; tumor suppressor; IAP; stem cells; lymphoma]

Supplemental material is available at http://www.genesdev.org.

Received July 15, 2010; revised version accepted August 30, 2010.

Cell death by apoptosis is an active cell suicide process that serves to eliminate unwanted and potentially dangerous cells during development and tissue homeostasis (Thompson 1995; Jacobson et al. 1997; Meier et al. 2000; Danial and Korsmeyer 2004). Acquired resistance toward apoptosis is one of the hallmarks of cancer, and virtually all current cancer therapeutics kill by inducing apoptosis (Hanahan and Weinberg 2000; Reed and Pellecchia 2005; Mehlen and Puisieux 2006; Degenhardt and White 2006). However, we still know very little about the precise stages and cellular context in which apoptosis limits the development and/or progression of malignancies. In particular, much remains to be learned about the physiological role of apoptosis, if any, in restricting the numbers of normal stem cells and preventing the emergence of cancer stem cells (Oguro and Iwama 2007). The idea that cancer arises from stem cells is attractive because it explains many properties of tumors (Reya et al. 2001; Passegue et al. 2003; Clarke and Fuller 2006; Rossi et al. 2008). Given the large body of work showing an association between apoptosis and cancer, it is somewhat surprising that only very few proteins with a direct function in apoptosis are known tumor suppressors (Scott et al. 2004). Therefore, investigating the physiological function of specific cell death proteins with respect to tumor suppression and stem cell apoptosis remains an important area of active investigation.

Inhibitor of Apoptosis Proteins (IAPs) are a family of prosurvival proteins that have been conserved from insects to humans (Salvesen and Duckett 2002; Vaux and Silke 2005). Many IAPs act as E3 ubiquitin ligases to target key cell death proteins, including caspases and themselves, for proteasome-mediated degradation (Yang et al. 2000; Vaux and Silke 2005; Schile et al. 2008). Because IAPs are frequently overexpressed in human tumors, they have become important pharmacological targets for developing new anti-cancer drugs (Reed 2003; LaCasse et al. 2008). In cells that are doomed to die, IAPs are negatively regulated by natural IAP antagonists that were originally identified in *Drosophila* (Kornbluth and White 2005; Steller 2008). Although the proteins encoded by these genes share overall very little protein homology, they all contain a short N-terminal peptide motif—termed IBM (IAP-binding-motif)—that is required for IAP binding and cell killing (Shi 2004). Whereas deleting the *Drosophila* IAP antagonists Reaper, Hid, and Grim blocks apoptosis in the fly, inactivation of either Smac/DIABLO, Omi/HtrA2, or both together in double-mutant mice did not lead to increased resistance toward cell death or increased tumor formation (White et al. 1994; Okada et al. 2002; Jones et al. 2003; Martins et al. 2004). Therefore, a physiological role of these proteins remains to be established.

Another mammalian IAP antagonist is ARTS, which is localized to mitochondria in living cells (Larisch et al.

[4]Corresponding author.
E-MAIL steller@rockefeller.edu; FAX (212) 327-7076.
Article is online at http://www.genesdev.org/cgi/doi/10.1101/gad.1970110.

2000). ARTS (Sept4_i2) is a splice variant of the *Sept4* septin gene, and is unique among septins with respect to its proapoptotic activity and ability to bind IAPs (Larisch et al. 2000; Macara et al. 2002; Gottfried et al. 2004). Although ARTS contains no detectable IBM, it binds efficiently to XIAP (Gottfried et al. 2004). Significantly, expression of ARTS is frequently lost in human leukemia, indicating that ARTS may function as a tumor suppressor (Elhasid et al. 2004). In order to further examine the physiological function of ARTS, we generated mice deficient for the *Sept4* gene (Kissel et al. 2005). Here we show that *Sept4*-deficient mice exhibit increased incidence of hematopoietic malignancies. The loss of *Sept4* function both promotes spontaneous leukemia/lymphoma and accelerates lymphoma development in an Eμ-*Myc* background. In addition, ARTS mRNA expression is significantly reduced in many human lymphoma patients, demonstrating that down-regulation of ARTS is not restricted to leukemia. Moreover, *Sept4*-deficient mice have increased numbers of hematopoietic stem and progenitor cells (HSPCs) that express elevated levels of XIAP protein in doomed cells. Although lymphocytes and other differentiated cells in *Sept4*-null mice have no detectable defects in apoptosis, mutant HSPCs are significantly more resistant to apoptotic stimuli, such as X-ray irradiation. Inactivation of XIAP partially suppresses the stem cell and tumor phenotypes of *Sept4*-null mice. These findings indicate that *Sept4*/ARTS functions as a tumor suppressor that regulates the HSPC pool size by inducing apoptosis via XIAP inhibition. More generally, our results suggest that apoptosis plays an important role as a frontline defense against cancer by restricting the number of normal stem cells, and that defects in stem cell apoptosis contribute to the emergence of cancer stem cells.

Results

Sept4-*null mice develop spontaneous hematopoietic malignancies*

In order to investigate the physiological role of the proapoptotic ARTS protein, we generated a mouse line with a deletion in the *Sept4* gene, which encodes ARTS (Kissel et al. 2005). *Sept4*-null mice lack the annulus and have defects in the caspase-mediated elimination of bulk cytoplasm during spermiogenesis, resulting in male sterility (Kissel et al. 2005). Besides ARTS, *Sept4* encodes other protein isoforms that have been implicated in traditional septin functions, such as organization of actin filaments and cytokinesis (Hall and Russell 2004; Kim et al. 2004; Ihara et al. 2005; Spiliotis et al. 2005; Kinoshita 2006; Barral and Kinoshita 2008; Weirich et al. 2008). However, these functions appear to be largely redundant due to the presence of closely related septin genes (Ihara et al. 2005, 2007; Kissel et al. 2005; Iwasako et al. 2008). Significantly, only ARTS has the ability to bind to IAPs and promote apoptosis in cell-based assays, and expression of ARTS, but not the conventional H5 (Sept4_i1) septin isoform, is selectively lost in the majority of acute lymphoblastic leukemia (ALL) patients (Elhasid et al. 2004; Gottfried et al. 2004). Since these results suggest a tumor suppressor function of ARTS, we surveyed *Sept4*-null mice for development of tumors. The incidence of spontaneous hematopoietic malignancies dramatically increased in 11- to 15-mo-old *Sept4*-null mice when compared with their wild-type littermates (Fig. 1A; Supplemental Table 1). Although a mild hyperplasia was detected in some wild-type mice, none of them developed neoplasia. In contrast, approximately one-third of our $Sept4^{-/-}$ mutants and almost 10% of the $Sept4^{+/-}$ mice developed spontaneous neoplasias (Supplemental Table 1). Most tumors from $Sept4^{+/-}$ mice retained ARTS expression, demonstrating that the remaining wild-type *Sept4* allele was not lost or silenced (Supplemental Fig. 1C). This suggests a modest haploinsufficiency of *Sept4* for tumor suppression.

We also observed some spontaneous tumors in other tissues, but the considerable variation and slow onset (10–14 mo) of tumor formation made it difficult to systematically analyze these cases (data not shown). Within the hematopoietic system, neoplasias were not restricted to a specific cell type, and we also observed splenomegaly in some $Sept4^{-/-}$ mice (Fig. 1; Supplemental Fig. 1A,B; Supplemental Table 1). Our results provide genetic evidence for a tumor suppressor function of the *Sept4* locus.

Sept4-*null mice have increased numbers of hematopoietic stem cells (HSCs)*

To better characterize the development of malignancies in *Sept4* mutant mice, we looked for evidence of increased

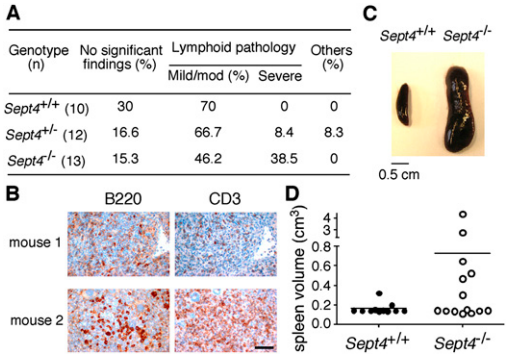

Figure 1. Loss of *Sept4* function leads to spontaneous hematopoietic malignancies. (*A*) Summary evaluation of lymphoid pathologies. Mice of the indicated genotypes were aged to 11–15 mo and were histopathologically evaluated. A significant fraction of *Sept4* mutant animals displayed neoplasia, whereas wild-type controls developed only mild lymphoid hyperplasia. (mod) Moderate; (Others) mice with pathologies unrelated to the hematopoietic system. (*B*) Immunohistochemistry of lymph node paraffin sections from two *Sept4*-deficient mice that developed lymphoma, showing a high number of B cells ($B220^{pos}$) and T cells ($CD3^{pos}$). Bars, 60 μm. (*C*) Representative photograph showing the enlarged spleen of a *Sept4*-null mouse, which developed spontaneous lymphoma, compared with an age-matched wild-type animal. (*D*) Histogram displaying the spleen size distribution in 11- to 15-mo-old wild-type and *Sept4*-null mice. Each dot corresponds to one mouse, and the line indicates the mean value.

proliferation in the lymphocyte population. No evidence for increased proliferation of lymphocytes that might explain the formation of malignancies was observed (Supplemental Fig. 2). If anything, it appeared that proliferation of *Sept4*-deficient T cells was slightly slower than that of wild-type cells. Therefore, *Sept4* may play some role for efficient completion of the cell cycle, consistent with the known function of septins in cytokinesis (Neufeld and Rubin 1994; Longtine et al. 1996; Adam et al. 2000; Hall and Russell 2004). However, since the number of T cells in vivo was not affected by the loss of *Sept4* function, it is unlikely that the very slight retardation in the proliferation of activated T cells is responsible for the increased tumor incidence of *Sept4* mutants (Supplemental Fig. 3).

Analysis of the cellular composition of the main lymph organs (thymus, spleen, and bone marrow [BM]) in young (6- to 13-wk-old) mice showed overall similar total cellularity in *Sept4*-deficient and wild-type littermates (Fig. 2A). To get more insight into the lymphoid phenotype of $Sept4^{-/-}$ mice, flow cytometry experiments with fluorescent surface markers were performed with cell suspensions from the spleen, thymus, and BM. In these studies, B and T cells showed a similar distribution for knockout and wild-type littermates (Supplemental Fig. 3). However, even though the number of mature B cells ($B220^{high}IgM^{pos}$) was normal, we found an increased number of B-lineage progenitor ($B220^{low}IgM^{neg}$) and immature B ($B220^{low}IgM^{pos}$) cells in the BM of *Sept4*-deficient mice (Fig. 2B). Next, we examined the HSC pool and found a significant increase (~1.5-fold) in $Lin^{neg}Sca1^{pos}ckit^{pos}$ (LSK) cells in the BM of young (6- to 13-wk-old) *Sept4*-deficient mice (Fig. 2C; Kondo et al. 2003). The increased LSK numbers persisted and were even more evident in 11- to 15-mo-old *Sept4*-null mice, likely due to an accumulation of LSK cells in the BM over time (Fig. 2C; Morrison et al. 1996).

To further quantify the number of stem cells in wild-type and *Sept4*-null mice, we performed the competitive repopulating unit (CRU) functional assay using the congenic CD45.1/CD45.2 system (Spangrude et al. 1988; Szilvassy and Cory 1993). Various limiting dilutions of donor BM test cells of either $Sept4^{+/+}$ or $Sept4^{-/-}$ CD45.2 mice were transplanted together with 200,000 CD45.1 BM cells into lethally irradiated CD45.1 mice. Peripheral blood from the recipient CD45.1 mice was collected 16 wk after transplantation to assess the CD45.2 hematopoietic repopulation, and CRU numbers were calculated (Fig. 3A,B). These experiments revealed a more than twofold increase in CRU frequency (one in every 175,720 total BM cells for $Sept4^{+/+}$ mice vs. one in every 62,662 total BM cells for $Sept4^{-/-}$ mice), demonstrating that the loss of *Sept4* function causes a significant increase ($P = 0.0127$) in the number of HSCs. This result is in overall agreement with the observed increase of LSK cells in the BM of *Sept4*-null mice. Moreover, it shows that these extra cells are functional stem cells that have the ability to repopulate the entire lymphoid and myeloid system. The LSK content in the BM of the recipient mice was also analyzed 16 wk after transplantation. As observed with complete *Sept4*-null mice, the percentage of LSK cells was higher when the BM of CD45.1 host mice was repopulated by CD45.2 $Sept4^{-/-}$ cells compared with wild-type cells (Fig. 3C), indicating a cell-autonomous function of *Sept4*.

The observed increase in the number of HSPCs could be the result of either increased proliferation or decreased apoptosis. To address the former, we examined the growth

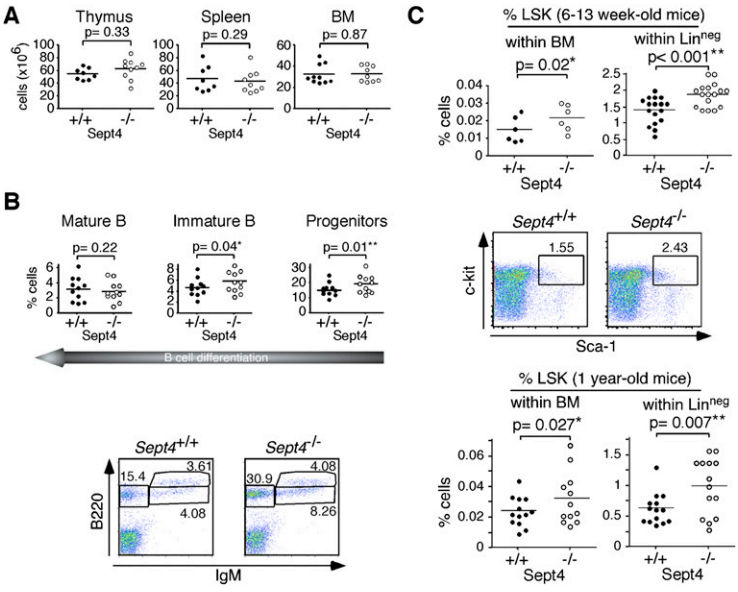

Figure 2. $Sept4^{-/-}$ mice have increased numbers of HSPCs in the BM. (*A*) Evaluation of cellular composition in lymph organs of $Sept4^{+/+}$ and $Sept4^{-/-}$ mice in 6- to 13-wk-old mice (paired *t*-test). Loss of Sept4 function did not lead to overt changes in the total cellularity in the thymus, spleen, and BM. (*B*) Flow cytometry analysis of B-cell lineage in the BM of $Sept4^{+/+}$ and $Sept4^{-/-}$ mice. Progenitor cell ($B220^{low}IgM^{neg}$) and immature B cell ($B220^{low}IgM^{pos}$) percentages were significantly higher in $Sept4^{-/-}$ mice versus their $Sept4^{+/+}$ counterparts (paired *t*-test). No significant differences were found in mature B-cell numbers ($B220^{high}IgM^{pos}$). A representative FACS analysis is shown *below*. Each dot in the graphs in *A* and *B* indicates the value obtained from a single mouse, and the lines show the mean value for each group. Numbers in the *bottom* panel of *B* indicate the percentage of cells within the gated subpopulation. (*C*) Flow cytometry graph showing the percentage of LSK cells in total BM and within the Lin^{neg} cell fraction in young (*top* panel) and old (*bottom* panel) mice. A significantly higher percentage of LSK cells was detected in the BM of $Sept4^{-/-}$ compared with $Sept4^{+/+}$ mice (paired *t*-test). Each dot indicates the value obtained from a single mouse, and the lines represent the mean value for each group. A representative FACS analysis of Lin^{neg} cells obtained from the BM of young $Sept4^{+/+}$ and $Sept4^{-/-}$ littermates is represented in the *middle* panel. Numbers indicate the percentage of cells within the gated subpopulation.

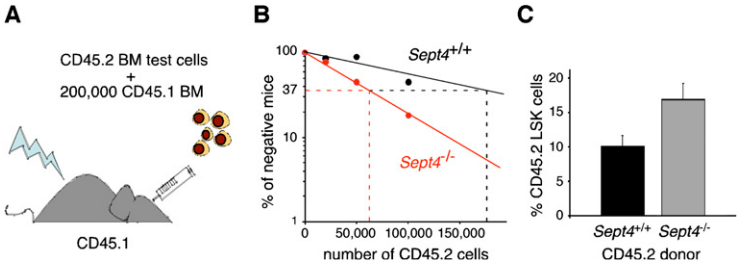

Figure 3. *Sept4*$^{-/-}$ mice have increased numbers of functional HSCs. (*A*) Diagram of the transplantation protocol. Different dilutions of CD45.2 BM cells from *Sept4*$^{+/+}$ or *Sept4*$^{-/-}$ mice were transplanted together with 200,000 CD45.1 BM cells into lethally irradiated CD45.1 mice. Orbital blood was taken 16 wk post-transplantation to monitor CD45.2 reconstitution. (*B*) Graph representing the percentage of recipient mice that failed reconstitution 16 wk after transplantation for a given number of *Sept4*$^{+/+}$ or *Sept4*$^{-/-}$ BM CD45.2 cells. *Sept4*$^{-/-}$ mice showed a significant increase in the CRU, indicative of higher numbers of functional HSCs. The chart corresponds to the pooled data from three independent experiments (n = 7–11 mice per genotype for each dilution; one-tailed; [*] P = 0.0127). (*C*) Lethally irradiated CD45.1 mice transplanted with 20,000 CD45.2 *Sept4*$^{+/+}$ or *Sept4*$^{-/-}$ BM cells and 200,000 CD45.1 BM cells were sacrificed 16 wk post-transplantation. Mice that received *Sept4*$^{-/-}$ BM cells showed an increase in the percentage of CD45.2 cells within the LSK population (P = 0.06; n = 3), indicating that BM cells from *Sept4*-null mice are more potent than wild-type cells in repopulating the BM.

rate and cell cycle progression of B-cell progenitors and LSK cells in *Sept4*-null and wild-type mice. We could not find any evidence for increased cell proliferation of B-cell progenitors and LSK cells in *Sept4* mutants (Supplemental Fig. 4). Therefore, increased proliferation does not appear to account for the accumulation of HSPCs.

Role of Sept4/*ARTS in apoptosis of HSPCs*

Since ARTS has been implicated in apoptosis, we examined whether the loss of *Sept4* function affects the apoptotic response of different cell types. To our surprise, we did not detect any significant apoptosis defects caused by the absence of *Sept4* function in differentiated lymphocytes (Fig. 4). Since ARTS has been reported to target IAPs, including XIAP, and because loss of XIAP function causes apoptotic phenotypes only in certain cell types (Schile et al. 2008), we decided to analyze apoptosis of lymphoid progenitor and stem cells. For this purpose, we isolated B220^{low}IgM^{neg} B-cell progenitors by cell sorting and cultured them for 6 h in the absence of growth factors and cytokines to induce apoptosis (Vaux et al. 1992; Dorsch and Goff 1996). As shown in Figure 5A, growth factor deprivation-induced apoptosis, as evaluated by TUNEL staining, was significantly reduced in *Sept4*-null cells compared with controls.

Next, we asked whether the loss of *Sept4* function provides a genuine survival advantage to HSPCs. Since doomed cells that are prevented from undergoing apoptosis can often die by different mechanisms, such as necrotic death, the reduced TUNEL staining that we observed in Figure 5A alone is no guarantee of true cell survival. Therefore, we analyzed the sensitivity to apoptosis in hematopoietic progenitors by using the colony-forming unit colony (CFU-C) assay (Miller et al. 2008). BM cultures were irradiated to induce apoptosis and plated in CFU-C medium. The number of CFU-Cs generated after 1 wk was significantly reduced in wild-type but not *Sept4*$^{-/-}$ BM cultures compared with nonirradiated cells (Fig. 5B,C). This demonstrates that the deletion of the *Sept4* gene protects hematopoietic progenitors from irradiation-induced apoptosis and permits true long-term cell survival.

In order to determine whether the loss of *Sept4* also protected LSK cells from apoptosis, which could readily explain their increased numbers, we performed both in vivo and ex vivo assays. *Sept4* wild-type and knockout

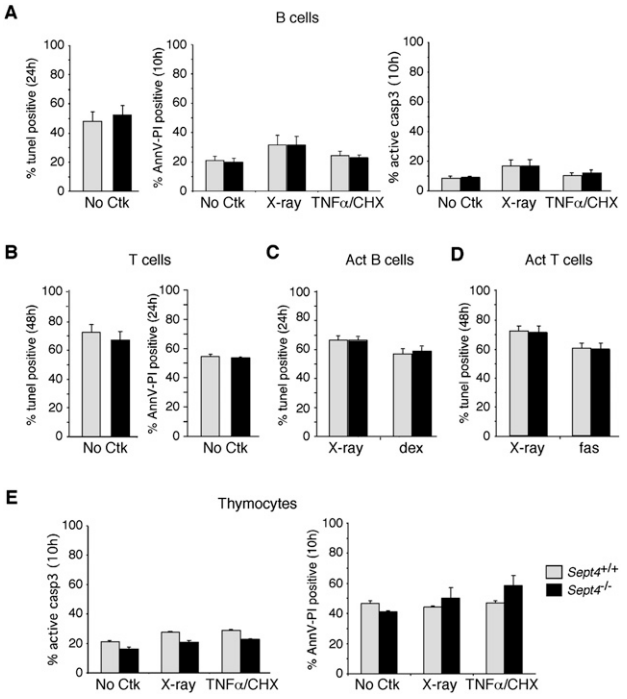

Figure 4. Loss of *Sept4* function does not affect lymphocyte apoptosis. Graphs represent the percentage of apoptotic cells detected as AnnexinV-PI or TUNEL-positive cells. (*A*) Apoptosis of B cells in response to cytokine withdrawal, X-ray irradiation, and TNFα/CHX, as well as caspase-3 activity were evaluated. Similar analyses were performed for T cells (*B*), LPS-activated B cells (*C*), concanavalin A-activated T cells (*D*), and thymocytes (*E*) for different paradigms. No differences in the response to apoptosis were observed for B cells or activated B and T cells. *Sept4*-null thymocytes showed reduced caspase 3 activation, but the rate of apoptosis, as assessed by AnnexinV-PI staining, was not different from wild type (No Ctk) no cytokines or growth factors; (CHX) cycloheximide; (fas) fas-ligand; (dex) dexamethasone. n = 4–7; mean ± SEM is represented; paired t-test.

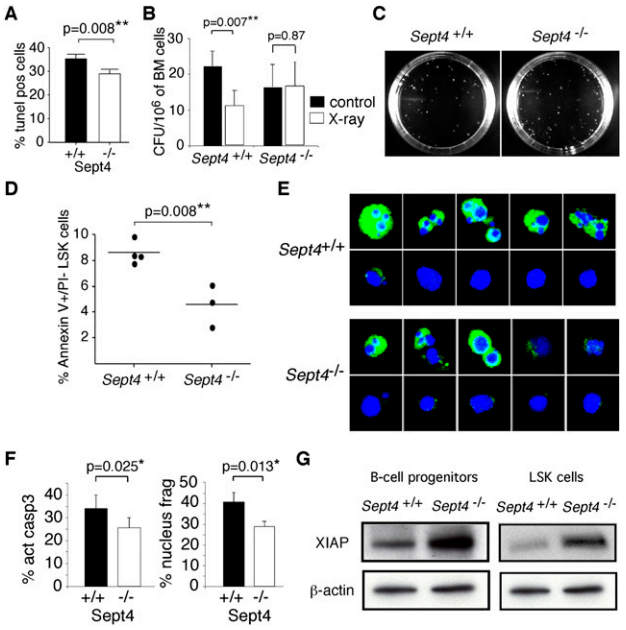

Figure 5. Loss of *Sept4* function protects HSPCs from apoptosis. (*A*) Histogram representing the percentage of apoptotic (TUNEL-positive) $B220^{pos}IgM^{neg}$ lymphoid progenitors after 6 h of growth factor deprivation (paired *t*-test). (*B*) Histogram comparing the number of CFU-Cs per 10^6 $Sept4^{+/+}$/$Sept4^{-/-}$ BM cells in response to X-ray irradiation (3 Gy). Nonirradiated plates were used as controls (paired *t*-test). Loss of *Sept4* function protected hematopoietic progenitors from irradiation-induced death ($n = 5$ experiments, each value is the average of a duplicated). (*C*) Representative examples of CFU-C assays from BM cultures 1 wk after X-ray irradiation (3 Gy). (*D*) Graphs representing the percentage of apoptotic LSK cells, defined as $AnnexinV^+/PI^-$, obtained from the BM of irradiated $Sept4^{+/+}$ and $Sept4^{-/-}$ mice (6 h after 6.5 Gy X-ray). $Sept4^{-/-}$ LSK cells were twofold more resistant toward radiation-induced apoptosis. Each dot corresponds to one mouse, and the lines represent the mean for each group. (*E*,*F*) Apoptosis in LSK cells sorted from $Sept4^{+/+}$and $Sept4^{-/-}$ mice and subjected directly to X-ray irradiation (8 Gy). (*E*) Representative examples of immunostained LSK cells showing caspase 3 activity (green) 4 h after irradiation. Nuclear fragmentation in apoptotic cells was detected using DAPI (blue). Individual cells from one experiment are shown in separate panels to allow a higher magnification. (*F*) Histogram showing the percentage of LSK cells displaying caspase 3 activity and nuclear fragmentation in response to radiation. Both indicators of apoptosis were decreased in LSK cells isolated from $Sept4^{-/-}$ compared with $Sept4^{+/+}$ mice ($n = 5$ experiments; values were obtained by calculating the average of measures in 10 random pictures obtained from each experiment). (*G*) Loss of *Sept4* function leads to increased XIAP protein levels. Western blot analysis of XIAP protein in lymphoid progenitors and cultured LSK cells after inducing apoptosis by either growth factor deprivation or X-ray irradiation. β-actin protein was used as a loading control.

mice were semilethally irradiated, and their BM cells were extracted 6 h after the irradiation. The percentage of apoptotic LSK cells was analyzed and found to be reduced by half in *Sept4*-null mice (Fig. 5D). In addition, BM LSK cells were isolated, apoptosis was induced by X-ray irradiation, and activated caspase-3 immunocytochemistry and nuclear fragmentation was evaluated (Fig. 5E,F). By all of these criteria, we found that the loss of *Sept4*/ARTS function caused a significant reduction of LSK cell apoptosis. Since overexpression of ARTS can reduce XIAP levels (Gottfried et al. 2004), we asked whether the loss of *Sept4*/ARTS function would lead to increased levels of XIAP. Indeed, we observed elevated levels of XIAP in both growth factor-deprived *Sept4*-null B-cell progenitors and LSK cells (Fig. 5G). This is consistent with the idea that ARTS promotes degradation of XIAP during apoptosis, and that the absence of this protein leads to increased XIAP protein levels, which in turn inhibit caspases and apoptosis.

The *Sept4* gene encodes different isoforms through differential splicing, but only ARTS has the ability to bind to XIAP in vitro, reduce XIAP protein levels, and induce apoptosis upon overexpression in cultured cells (Gottfried et al. 2004). This suggests that the effects on apoptosis and XIAP observed here are due to the loss of ARTS function. Consistent with this idea, we found that ARTS mRNA is much more highly expressed in LSK and B-cell progenitors than the other *Sept4* isoforms (Supplemental Fig. 5). Collectively, these results support a physiological role of ARTS for regulating stem cell death by down-regulation of XIAP in vivo.

Loss of Sept4 *function accelerates Myc-driven lymphomagenesis*

Malignant transformation is a multistep process during which oncogenic mutations affecting cell cycle control cooperate with impaired apoptosis (Hanahan and Weinberg 2000; Pelengaris et al. 2002). For example, overexpression of c-myc cooperates with overexpression of the anti-apoptotic Bcl-2 protein in the development of lymphoma (Strasser et al. 1990). Since our earlier results supported a proapoptotic role of *Sept4*/ARTS in vivo, we expected the loss of *Sept4* function to accelerate the development of tumors in a mouse lymphoma model. To investigate this possibility, we crossed $Sept4^{-/-}$ mice with animals expressing the *c-Myc* oncogene under the control of the immunoglobulin heavy chain enhancer (Eμ-*myc*) (Adams et al. 1985; Harris et al. 1988; Sidman et al. 1993). As shown in Figure 6A, *Sept4* deficiency reduced the life expectancy of Eμ-*myc* mice by ~50% and dramatically increased the number of circulating leukocytes and the incidence of neoplasia (Fig. 6B,C). Furthermore, we also saw a significant reduction of survival in $Sept4^{+/-}$ heterozygotes, which was intermediate between the $Sept4^{+/+}$ and $Sept4^{-/-}$ backgrounds (Fig. 6A). This reveals a haploinsufficiency of the *Sept4* locus in this model. Analysis of lymph organs from *Sept4*/Eμ-*myc* mice before the onset of disease (4- to 5-wk-old) revealed significantly increased cell numbers in the BM and increased numbers of circulating white blood cells (Supplemental Fig. 6). In agreement with our previous results, the number of BM LSK cells was significantly increased in Eμ-*myc*/*Sept4*-null mice compared with Eμ-*myc* siblings in a wild-type background (Fig. 6D,E). We also

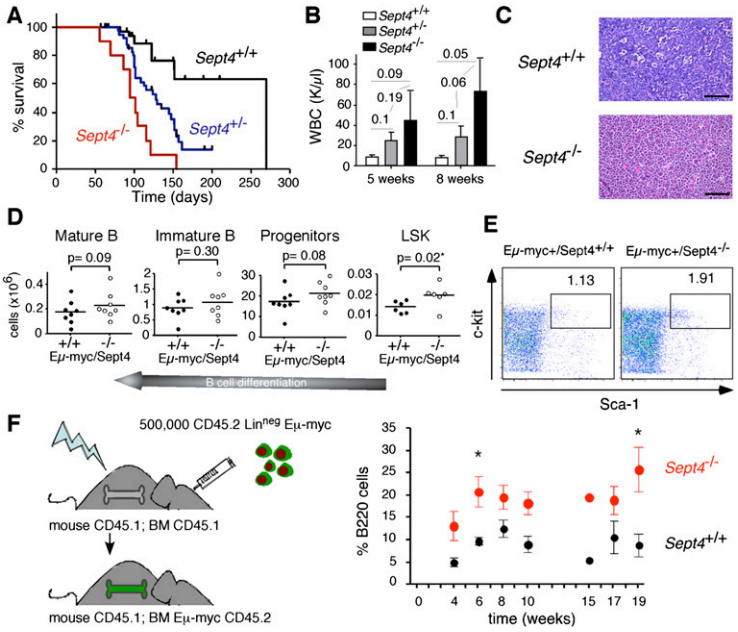

Figure 6. *Sept4* deficiency cooperates with c-*myc* in B-cell lymphomagenesis. (*A*) Kaplan-Meyer survival curves of Eμ-*myc* mice in different *Sept4* genetic backgrounds (*Sept4*$^{+/+}$, n = 40; *Sept4*$^{+/-}$, n = 43; *Sept4*$^{-/-}$, n = 10). (*B*) White blood cell (WBC) counts from Eμ-*myc* mice at 5 and 8 wk old. An increased number of circulating white blood cells was detected in *Sept4*$^{-/-}$ mice. Mean ± SEM is represented. The numbers correspond to the *P*-values (*t*-Student, nonpaired) (*Sept4*$^{+/+}$, n = 9; *Sept4*$^{+/-}$, n = 21; *Sept4*$^{-/-}$, n = 7). (*C*) Analysis of hematoxylin/eosin-stained thymus sections revealed that lymphoma developed much earlier in Eμ-*myc* mice lacking the *Sept4* gene (8-wk-old mice). Bars, 30 μm. (*D*) Flow cytometry study of total number of BM cells in different stages of lymphoid development in Eμ-*myc*/*Sept4* mice. LSK cell number was significantly higher in Eμ-*myc*/*Sept4*$^{-/-}$ mice compared with their Eμ-*myc*/*Sept4*$^{+/+}$ counterparts (4–5 wk old; paired *t*-test). Each dot corresponds to one mouse, and the lines indicate the mean value. (*E*) FACS example showing LSK frequency in the Lin^{neg} cell fraction obtained from the BM of Eμ-*Myc*/*Sept4* sibling mice. Numbers indicate the percentage of cells within the gated subpopulation. (*F*) Diagram of the transplantation protocol. CD45.2 Lin^{neg} Eμ-*myc*/*Sept4*$^{+/+}$ or Eμ-*myc*/*Sept4*$^{-/-}$ cells (500,000) were transplanted into a lethally irradiated CD45.1 mouse to completely reconstitute the BM with CD45.2 Eμ-*myc* cells. The graph on the *right* represents the percentage of CD45.2 B220^{pos} B-lineage cells in the peripheral blood at different times post-transplantation (n = 5/6 mice per genotype; mean and SEM are shown for each time point). Loss of *Sept4* function significantly accelerated the emergence of CD45.2 B220^{pos} B cells, indicating that *Sept4* functions cell-autonomously to restrict lymphoid hyperproliferation and lymphomagenesis.

investigated whether loss of *Sept4* function protects B cells from Myc-induced apoptosis, but found no evidence for this (Supplemental Fig. 6C). This is consistent with our earlier results revealing a preferential role of *Sept4*/ARTS in the regulation of apoptosis of stem and early progenitor cells. We also analyzed the cellular composition of tumors in Eμ-*myc Sept4* mice and found them to be mainly composed of primitive cells, similar to what has been described previously (Supplemental Fig. 6D; Strasser et al. 1990). Taken together, these results demonstrate that the loss of *Sept4* cooperates with c-*Myc* in lymphomagenesis.

The findings described so far suggest that *Sept4*-null mice develop malignancies due to increased resistance of their HSPCs to apoptosis. If so, this phenotype should be cell-autonomous to the lymphoid compartment, and not dependent on the genotype of the cellular environment. In order to test this prediction, we transplanted *Sept4*$^{+/+}$ or *Sept4*$^{-/-}$ Eμ-*myc* Lin^{neg} CD45.2 cells into lethally irradiated wild-type CD45.1 mice to completely reconstitute the recipient hematopoietic system with Eμ-*myc* CD45.2 cells (Fig. 6F). Peripheral blood was obtained at different times after transplantation to follow the accumulation of B cells (B220^{pos}). As observed in *Sept4*/Eμ-*myc* mice, we again found that the loss of *Sept4* function accelerated lymphomagenesis under these conditions (Fig. 6F). Therefore, *Sept4* plays a cell-autonomous role in suppressing lymphomagenesis in this model. Collectively, our results suggest ARTS functions as a tumor suppressor by promoting apoptosis of HSCs.

Inactivation of XIAP *suppresses* Sept4-*null mutant phenotypes*

Cell culture experiments suggest that the proapoptotic ARTS protein induces apoptosis, at least in part, by binding to and inhibiting XIAP (Gottfried et al. 2004). In addition, we observed increased levels of XIAP in *Sept4*-null cells (Fig. 5G), suggesting that *Sept4* plays a physiological role in regulating XIAP protein levels. In order to further explore whether XIAP is a major physiological target for the proapoptotic and tumor suppressor function of *Sept4*/ARTS, we generated double-mutant *Sept4*$^{-/-}$; *XIAP*$^{-/-}$ animals and examined sensitivity toward cell death and tumor formation (Fig. 7). We found that the resistance of *Sept4*-null HSPCs to apoptosis is suppressed by the loss of XIAP function in *Sept4/XIAP* double-knockout mice (Fig. 7A). In addition, the loss of XIAP also abolished the cell-autonomous lymphoproliferation seen in *Sept4*-null mice (Fig. 7B). Finally, inactivation of *XIAP* also suppressed the increased mortality of *Sept4*-null mice in the Eμ-*myc* tumor model (Fig. 7C). As reported previously, loss of XIAP function significantly extended life expectancy in the Eμ-*myc* mouse model (Schile et al. 2008), and the loss of *Sept4*/ARTS was inconsequential under these conditions. These results indicate that XIAP is a major physiological target for the proapoptotic and tumor suppressor activity of ARTS.

Discussion

It is generally accepted that cell death by apoptosis plays an important role in preventing tumor development, and

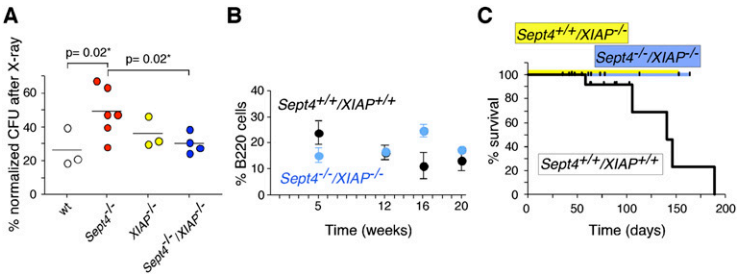

Figure 7. Loss of XIAP function suppresses *Sept4*-null phenotypes. Epistasis analysis using double-mutant combinations for *XIAP* and *Sept4*. (*A*) The resistance of *Sept4*-null HSPCs to apoptosis is suppressed by the loss of XIAP function in *Sept4/XIAP* double-knockout mice. Graph showing the percentage of CFU-Cs 1 wk after inducing apoptosis by X-ray irradiation (3 Gy), normalized to the number of CFU-Cs present in non-irradiated plates. Each dot corresponds to one mouse, and the lines indicate the mean value for each group (paired *t*-test; each value is the average of a duplicated). (*B*) Loss of XIAP function abolishes the accelerated cell-autonomous lymphoproliferation seen in *Sept4*-null mice (Fig. 6F). Lethally irradiated wild-type CD45.1 mice were transplanted with 200,000 CD45.2 Lin^{neg} Eμ-myc cells either wild type or deficient for *Sept4/XIAP* genes. The graph represents the percentage of CD45.2 $B220^{pos}$ B cells in the peripheral blood over the time after transplantation. Unlike the accelerated lymphoproliferation seen with *Sept4*-null LSK cells, no significant differences were found when mice were transplanted with either wild-type or double-knockout Eμ-*myc* LSK cells, indicating that inactivation of *XIAP* suppresses the accelerated lymphoproliferation of *Sept4*-null LSK cells ($n = 4$–6 mice per genotype; mean and SEM are represented for each time point). (*C*) Kaplan-Meyer survival curves of Eμ-*myc* mice in different *Sept4* and *XIAP* genetic backgrounds. The loss of the *Sept4* gene did not increase the mortality of Eμ-myc mice when the *XIAP* gene was deleted too ($Sept4^{+/+}/XIAP^{+/+}$, $n = 17$; $Sept4^{+/+}/XIAP^{-/-}$, $n = 6$; $Sept4^{-/-}/XIAP^{-/-}$, $n = 9$) (cf. Fig. 6A). Taken together, these results indicate that XIAP is a major physiological target for the proapoptotic and tumor suppressor activities of ARTS.

considerable efforts are being devoted to exploit advances in apoptosis research for the development of new cancer therapeutics (Fesik 2005; Reed and Pellecchia 2005; LaCasse et al. 2008). One important family of anti-apoptotic proteins that has attracted considerable attention as potential drug targets in cancer therapy is the IAPs, which can directly inhibit caspases, the key executioners of apoptosis (Salvesen and Duckett 2002; Vaux and Silke 2005; Schile et al. 2008). However, genetic inactivation of the mammalian IAP antagonists Smac/DIABLO and Omi/HtrA2 has failed to reveal any physiological requirement of these IAP-binding proteins in apoptosis, IAP regulation, or tumor suppression (Okada et al. 2002; Jones et al. 2003; Martins et al. 2004). One possible explanation for the lack of overt mutant phenotypes is the potential functional redundancy of different IAP antagonists in the mouse. This would not be surprising given the well-documented partially redundant function of different IAP antagonists in *Drosophila* (Steller 2008). In this study, we investigated the role of the IAP antagonist ARTS for cell death and tumor formation by analyzing *Sept4*-null mice (Kissel et al. 2005). The *Sept4* gene encodes both "conventional" septins and the proapoptotic ARTS protein (Larisch et al. 2000; Macara et al. 2002). Previous studies have shown that overexpression of ARTS can reduce XIAP protein levels and induce apoptosis in cultured cells, and that ARTS expression is selectively lost in human ALL patients (Larisch et al. 2000; Elhasid et al. 2004; Gottfried et al. 2004). It has also been reported that *Sept4* is underexpressed in human acute myeloid leukemia (AML) patients (Santos et al. 2010), and we found that ARTS mRNA is reduced in a significant portion of human lymphoma patients (data not shown). Significantly, loss of *Sept4* function promotes hematopoietic malignancies in the mouse, providing genetic evidence for a tumor suppressor function of this gene. Previous studies reported an association between an increased HSC pool and myelodysplasia followed by the development of both ALL and AML (Domen et al. 2000; Yilmaz et al. 2006). Therefore, we carefully examined *Sept4*/ARTS-null mice for myeloid phenotypes but did not detect any. Since distinct genes were manipulated in these different studies, it appears that not all pathways that regulate the HSC pool will generate a cancer within the myeloid lineage, and more work is needed to clarify whether myelodysplastic syndrome is strictly a stem cell disorder (Nimer 2008).

Given the proposed proapoptotic role of ARTS and the increased tumor incidence in *Sept4*-null mice, we expected to see widespread apoptosis defects in *Sept4*-null mice. However, no cell death abnormalities were observed in a wide range of differentiated cells exposed to many different apoptotic stimuli (Fig. 4). On the other hand, HSPCs from *Sept4*-null mice were significantly more resistant toward apoptosis than their wild-type counterparts and showed a robust increase in true clonogenic cell survival (Fig. 5A–F). The observed twofold increase in LSK cell survival (Fig. 5D) is comparable with what has been reported for the loss of p53 or elevated levels of Bcl-2 expression (Domen et al. 2000; Liu et al. 2009). Furthermore, we found that *Sept4*-deficient mice have increased numbers of HSCs, as indicated by both the use of markers and transplantation experiments testing for the presence of functional stem cells by reconstituting the hematopoietic system of lethally irradiated recipient mice (Fig. 3). Since we found no evidence whatsoever of increased cell proliferation in *Sept4*-null mice, it appears that the elevated numbers of functional stem cells are due to impaired stem cell apoptosis.

We observed accelerated tumor development in *Sept4* mutants and used transplantation experiments to show that this reflects a cell-autonomous requirement for this gene to restrict malignancies (Fig. 6). We attribute both the proapoptotic and tumor suppressor functions of the *Sept4* gene to the loss of ARTS, and not the other protein isoforms derived from this locus, for several reasons.

First, ARTS is the most abundant isoform in HSPCs (Supplemental Fig. 5) and is the only one with a known ability to bind to XIAP and induce apoptosis (Gottfried et al. 2004). Second, expression of ARTS, but not the related septin isoform H5, is selectively lost in human ALL patients (Elhasid et al. 2004). Third, we found that mutant HSPCs retained elevated levels of XIAP protein compared with wild-type controls in response to apoptotic stimuli (Fig. 5G). It has been reported previously that overexpression of ARTS, but not the related septin isoforms, can promote the degradation of XIAP by ubiquitin–proteasome-mediated protein degradation (Gottfried et al. 2004). Therefore, the elevated XIAP levels we observe are likely the result of decreased XIAP protein degradation due to the absence of ARTS in *Sept4*-null mice. Finally, we used epistasis analysis to investigate if XIAP is a physiological target for the proapoptotic and tumor suppressor activities of Sept4/ARTS (Fig. 7). The loss of XIAP function suppressed several of the apoptosis and tumor-related phenotypes observed in *Sept4*-null animals, including resistance toward X-ray-induced cell death, increased cell-autonomous lymphoproliferation, elevated tumor incidence, and mortality in the Eμ-*myc* model (Fig. 7). We conclude that XIAP is an important physiological target for the proapoptotic and tumor suppressor function of ARTS.

Since no apoptotic phenotypes were observed for differentiated lymphocytes and thymocytes in either *XIAP* or *Sept4* mutant mice, it appears that XIAP-mediated regulation of caspases plays a nonredundant role at the progenitor stage, but is less critical for differentiated cell types. We also observed a slight delay in the proliferation of activated *Sept4*-null T cells in vitro, fewer cycling-activated B cells, and slightly decreased BrdU incorporation of LSK cells in vivo (Supplemental Figs. 2, 4), suggesting a modest nonredundant role of *Sept4* for efficient cycling. Since septins are important for cytokinesis in yeast and *Drosophila*, the observed defects presumably reflect a requirement of the "conventional" septin function of this locus in this context (Neufeld and Rubin 1994; Cvrckova et al. 1995; Longtine et al. 1996; Adam et al. 2000; Kremer et al. 2007; Barral and Kinoshita 2008). We believe that cell cycle defects in *Sept4*-null mice are not more pronounced due to the presence of multiple genes encoding structurally related septin proteins with partially redundant function (Longtine et al. 1996; Hall et al. 2005; Spiliotis et al. 2005; Weirich et al. 2008). In any event, it appears highly unlikely that these mild cell cycle defects contribute to either the accumulation of LSK cells or increased tumor incidence in *Sept4*-null mice, since retarded growth, if anything, should produce the opposite phenotype. We also considered that the loss of *Sept4* function might lead to mitochondrial defects in HSPCs because loss of *Sept4* function causes mitochondrial structural defects in spermatids (Kissel et al. 2005). However, no differences in the mitochondrial ultrastructure were detected in various somatic cells, including hepatocytes and Lin^- cells isolated from BM (Supplemental Fig. 7; Kissel et al. 2005). Taken together, these observations support a physiological function of ARTS as an IAP antagonist regulating apoptosis of HSPCs, and for tumor suppression in the mouse.

We propose that ARTS functions as a tumor suppressor that regulates HSPC pool size by inducing apoptosis of superfluous stem cells. According to this model, loss of proapoptotic ARTS function promotes tumorigenesis in two distinct ways. First, loss of ARTS-mediated apoptosis leads to increased numbers of normal HSPCs. If cancer indeed arises from stem cells, elevated numbers of normal HSPCs are expected to increase cancer risk due to the presence of the number of cellular targets available for transforming mutations (Passegue et al. 2003; Clarke and Fuller 2006; Tan et al. 2006; Rossi et al. 2008). Second, after these stem cells acquire transforming mutations and become "cancer stem cells," they are more likely to survive in the absence of ARTS due to increased resistance toward apoptosis. A combination of these two proposed mechanisms, over time, is expected to significantly increase tumor risk. Consistent with this model, we find that *Sept4* function is specific for cell death of HSPCs in the hematopoietic compartment; that loss of *Sept4* leads to genuine, long-term survival of HSPCs (Fig. 5); and that *Sept4* acts cell-autonomously to both regulate the number of functional stem cells and suppress tumor formation (Figs. 3, 6F). Furthermore, the observed cooperation of c-myc and loss of *Sept4* function in lymphomagenesis is qualitatively very similar to what has been described previously for overexpression of anti-apoptotic proteins such as Bcl-2 (Bissonnette et al. 1992; Strasser et al. 1990; Pelengaris et al. 2002). However, to the best of our knowledge, this is the first report demonstrating a physiological function for a gene encoding an IAP antagonist in apoptosis and tumor suppression. Because loss of *Sept4*/ARTS impairs apoptosis of HSPCs, but not of more differentiated cells, and because mutant HSPCs can generate tumors in an otherwise wild-type background, it appears that apoptosis serves to restrict the number of normal stem cells to prevent tumorigenesis. This suggests that apoptosis is a frontline defense against cancer that operates at the level of stem cells to prevent the survival of superfluous and potentially dangerous pluripotent stem and progenitor cells. Our results also illustrate the potential risks of introducing large numbers of stem cells for the purpose of tissue regeneration, since the sustained presence of abnormally high numbers of stem cells may dramatically increase the incidence of cancer.

Materials and methods

Mice

Sept-null and and *XIAP*-null mice were described previously (Harlin et al. 2001; Kissel et al. 2005). The apoptotic response of cells from *XIAP*-null and *XIAP*-ΔRING mice was virtually identical in several paradigms (Supplemental Fig. 2; Schile et al. 2008; AJ Schile and H Steller, unpubl.). Mice used in this study were backcrossed at least six times onto C57BL/6J. Sibling and same-gender mice were used when the paired *t*-test was applied. Eμ-*myc* mice were obtained from Jackson Laboratory [strain B6.Cg-Tg(IghMyc)22Bri/J].

Pathology analyses and survival curves

Gross necropsy was performed by the Genetically Engineered Mouse Phenotyping Core at Memorial Sloan-Kettering Cancer Center. Peripheral blood was sampled by retro-orbital bleeding at the animal care facility of The Rockefeller University. Cohorts of mice were monitored for survival over time before generating a Kaplan-Meier survival curve. The heterozygous mice were followed for only 200 d due to a technical problem. However, the *Sept4* wild-type and knockout mice were followed until none of them were alive.

Flow cytometry and cell analyses

Thymus, spleen, and BM (both tibiae and femur) single-cell suspensions were obtained in PBS/2% FBS buffer after ammonium chloride lysis of the red blood cells and straining through a nylon mesh. The total cell number was calculated using a standard hemocytometer. Surface marker expression was determined by FACS analysis after staining nonfixed cells for 25 min on ice with monoclonal antibodies. These antibodies were B220-APC, IgM-PE, IgD-FITC, CD19-FITC, CD90-PE, CD4-PE, CD8-FITC, Sca-1-PE, and c-kit-FITC (all from Becton Dickinson). To purify B-cell progenitors and LSK cells, BM cell suspensions were separated in two populations by depletion of mature hematopoietic cells and their committed precursors using a cocktail of biotinylated monoclonal antibodies conjugated to anti-biotin magnetic microbeads (Lineage Cell Depletion Kit, Miltenyi Biotec). This cocktail includes antibodies against CD5, CD45R (B220), CD11b, Anti-Gr-1 (Ly-6G/C), 7-4, and Ter-119. The lineage-positive cell population was used to sort B-cell progenitors ($Lin^{pos}B220^{pos}IgM^{neg}$), and the lineage-negative cell population was used to sort for hematopoietic LSK stem cells.

Transplantation assays

HSC quantitation was assessed by competitive repopulation assays using the congenic CD45.1/CD45.2 (Ly5.1/Ly5.2) system. Different numbers of total BM cells obtained from CD45.2 *Sept4*$^{+/+}$ or *Sept4*$^{-/-}$ mice were injected together with 2×10^5 CD45.1 total BM cells into lethally irradiated (10 Gy) CD45.1 mice. Peripheral blood was collected from recipient mice 16 wk post-transplantation. Red blood cells were lysed, and each blood sample was divided into three to analyze the reconstitution of B ($B220^{pos}$), T ($CD90.2^{pos}$), and myeloid (Mac-1/CD11b and Gr-1/Ly6G-Ly6C) lineages. A recipient mouse was scored as positive when ≥5% of CD45.2 cells were found within all three lineages. The percentage of recipients in each experimental group that failed reconstitution was plotted against the number of test cells transplanted, and Poisson statistics were applied to estimate the CRU within the donor cell population. The CRU frequency was calculated as the reciprocal of the number of test cells that yielded a 37% negative response.

For Eμ-myc cell transplantation experiments, 5×10^5 Lin^{neg} cells obtained from CD45.2 *Sept4*$^{+/+}$/*Sept4*$^{-/-}$ Eμ-*myc* mice were injected into lethally irradiated (10 Gy) wild-type CD45.1 mice to totally reconstitute the recipient hematopoietic system with CD45.2 Eμ-*myc* cells. Peripheral blood was collected at different times to analyze the percentage of CD45.2 $B220^{pos}$ cells.

Apoptosis assays

Double-positive $CD4^{pos}CD8^{pos}$ pre-T thymocytes were sorted from *Sept4* wild-type or knockout mice and cultured in RPMI-1640 medium supplemented with 10% FBS, L-glutamine, penicillin/streptomycin, and 2-β-mercaptoethanol (RPMI complete media). Resting B and T cells were isolated by magnetic cell sorting depletion (MACS; Miltenyi Biotec). LPS and IL-4 were used to activate B cells, and Concanavalin-2 and IL-2 were used to activate T cells. Concentrations of drugs to induce apoptosis were 20 nM etoposide, 10 ng/mL Fas-ligand plus 1 μL M2 antibody, 100 nM taxol, 8 Gy X-ray, and 10 nM dexamethasone.

B-cell progenitors were cultured for 6 h in RPMI complete media and growth factor deprivation conditions. TUNEL assays were then performed following the manufacturer's instructions (MBL, Mebstain) with some modifications. Cells were fixed with 3% PFA and permeabilized with 0.2% Triton-X in PBS (both steps for 15 min at room temperature). AnnexinV/PI staining followed the manufacturer's protocol (BD, 556419). Activated caspase 3 was determined by using the Casp3 Asp175 antibody (dilution 1:200; Cell Signaling, 9661) in fixed cells.

To study the effect of apoptosis in HSPCs, equal numbers of total BM cell were cultured in semisolid methylcellulose medium to grow CFU-Cs. The plates were irradiated with 3 Gy X-ray, and CFU-Cs were counted after 1 wk of incubation at 37°C and 5% CO_2. Nonirradiated plates were used as controls.

The in vivo assays to check the apoptotic sensitivity of LSK cells in the BM were performed by irradiating whole mice with 6.5 Gy X-ray. After 6 h, BM cells were obtained, and the percentage of apoptotic LSK cells was determined by staining them with surface markers and AnnexinV/PI, and by FACS analysis.

Immunoblotting

LSK cells were sorted as described before for staining purposes and cultured in a 35-mm Petri dish with 2 mL of SFEM media (Stem Cell Technologies, 09600) supplemented with 50 U/mL penicillin/streptomycin, 50 ng/mL rmSCF, 50 ng/mL rmTPO, 50 ng/mL rmFlt-3L, and 20 ng/mL rhIL-11 (all from Peprotech) for 48 h in a 37°C, 5% CO_2 incubator. After that, they were maintained in media with only 10 ng/mL rmSCF and 10 ng/mL TPO for another 48 h. The cells were then X-ray-irradiated (10 Gy) to induce apoptosis.

B-cell progenitors or LSK cells were homogenized in lysis buffer (320 mM sucrose, 10 mM Tris at pH 8.0, 3 mM $CaCl_2$, 2 mM $MgCl_2$, 0.1 mM EDTA at pH 8.0, 0.5% NP-40 supplemented with a tablet of proteases inhibitor cocktail[Roche]) after inducing apoptosis (as described above). Lysates were incubated for 30 min on ice and clarified by centrifugation at 2000 rpm at 4°C. Protein concentrations were measured using the Bradford assay, and equal amounts of protein extracts were separated by SDS-PAGE and blotted to activated PVDF membrane (Immobilon-P membrane, Millipore) for Western blot analysis. Monoclonal XIAP antibody (1:1000; clone 28; Becton Dickinson) was incubated overnight at 4°C. The β-actin antibody (1:10000; 30 min at room temperature; Sigma) was used as loading control. The signal for XIAP was detected with the West Femto chemiluminescent kit (Pierce Biotechnology) and with the regular ECL kit (GE Healthcare, RPN2209) for β-actin.

Immunostaining

Sorted LSK cells were cultured for 4 h at 37°C and 5% CO_2 in RPMI-1640 complete media after 8.60 Gy X-ray irradiation. Cells were then washed with PBS supplemented with 0.1 mM $CaCl_2$ and 1 mM $MgCl_2$, fixed in 3% paraformaldehyde, and permeabilized with PBS containing 0.2% Triton X-100. Afterward, they were incubated overnight with a rabbit anti-activated caspase-3 antibody (1:200 dilution; Cell Signaling, 9661). Cells were washed again and incubated for 1 h with a FITC-conjugated anti-rabbit antibody. The entire procedure was performed in a bottom-rounded 96-well plate. Finally, cells were cytospun onto

slides and mounted with VectaShield containing DAPI (Vector Laboratories).

Transcript analyses and quantitative RT–PCR

Poly(A^+) RNA was extracted using the Dynabeads mRNA Direct microkit as indicated by the manufacturer (Dynal). cDNA was immediately synthesized using MultiScribe Reverse Transcriptase (Applied Biosystems). Real-time PCR was performed using SYBR Green PCR master mix (Applied Biosystems) and the thermocycler conditions recommended by the manufacturer. PCRs were performed in triplicates in a total volume of 30 μL containing 2 μL of the reverse transcriptase reaction. Glucose 6-phosphate dehydrogenase mRNA (*G6PDH*) was used as control. Each sample was analyzed for *G6PDH* to normalize for RNA input amounts and to perform relative quantifications. For analysis of different murine *Sept4* transcripts, primers were designed using the computer program Primer Express (Applied Biosystems), and their composition was as follows: for *H5*: forward, 5′-TGGGATGGCAAGGGAACTC-3′, reverse 5′-GCCTG GCCACCCTTGTCT-3′; for *Cdcref2b*: forward, 5′-GCTGCAA CC ATGGATGATCA-3′, reverse 5′-GCCACAAGGA GCCTCT AAACTC-3′; for *M-septin*: forward, 5′-TGAAGCTGGGGATGA CAAGGA-3′, reverse 5′-CCACCAT GAGTGTAAAGTCAAAG C-3′; and for *ARTS*: forward, 5′-CAGGGCAGGGCTACC ACT AG-3′, reverse 5′- TGATGCAGGGCCTTCATGA-3′.

Statistical analyses

Data are presented as mean ± SEM. Experiments were analyzed by Student's *t*-tests, and *P*-values were considered statistically significant when $P < 0.05$ (*) or 0.01 (**). Sibling mice from the same gender and treated with exactly the same procedure were used for each pair when paired Student's *t*-test is indicated.

Acknowledgments

We thank Dr. T. Stoffel and members of Dr. A. Tarakhovsky's laboratory, especially Dr. I. Mecklenbräuker, for their advice; Dr. S. Mendez-Ferrer for his comments on the manuscript and help with the CRU experiments; and Dr. S. Barral for assisting with the statistical analyses. We are also grateful to the Comparative Pathology and Genetically Engineered Mouse Phenotyping and the Molecular Cytology Core facilities at Memorial Sloan Kettering Cancer Center, the Flow Cytometry Resource Center, The Comparative Bioscience Center (CBC), and the Electron Microscopy Resource Center at The Rockefeller University. M.G-F. was supported by a Caja Madrid Foundation Post-Graduate Fellowship and a generous gift from Fred and Stephanie Shuman. A.J.S. was a recipient of a Howard Hughes Medical Institute Predoctoral Fellowship, and H.S. is an Investigator with the Howard Hughes Medical Institute. Part of this work was supported by NIH grant RO1GM60124 to H.S., by the United States-Israel Binational Science Foundation, by a grant from the Tri-Institutional Stem Cell Initiative funded by the STARR Foundation, by an award from the Starr Cancer Consortium, and by the Empire State Stem Cell Fund through NYSDOH contract number C023046.

References

Adam JC, Pringle JR, Peifer M. 2000. Evidence for functional differentiation among *Drosophila* septins in cytokinesis and cellularization. *Mol Biol Cell* **11:** 3123–3135.

Adams JM, Harris AW, Pinkert CA, Corcoran LM, Alexander WS, Cory S, Palmiter RD, Brinster RL. 1985. The c-myc oncogene driven by immunoglobulin enhancers induces lymphoid malignancy in transgenic mice. *Nature* **318:** 533–538.

Barral Y, Kinoshita M. 2008. Structural insights shed light onto septin assemblies and function. *Curr Opin Cell Biol* **20:** 12–18.

Bissonnette RP, Echeverri F, Mahboubi A, Green DR. 1992. Apoptotic cell death induced by c-myc is inhibited by bcl-2. *Nature* **359:** 552–554.

Clarke MF, Fuller M. 2006. Stem cells and cancer: Two faces of eve. *Cell* **124:** 1111–1115.

Cvrckova F, De Virgilio C, Manser E, Pringle JR, Nasmyth K. 1995. Ste20-like protein kinases are required for normal localization of cell growth and for cytokinesis in budding yeast. *Genes Dev* **9:** 1817–1830.

Danial NN, Korsmeyer SJ. 2004. Cell death: Critical control points. *Cell* **116:** 205–219.

Degenhardt K, White E. 2006. A mouse model system to genetically dissect the molecular mechanisms regulating tumorigenesis. *Clin Cancer Res* **12:** 5298–5304.

Domen J, Cheshier SH, Weissman IL. 2000. The role of apoptosis in the regulation of hematopoietic stem cells: Overexpression of Bcl-2 increases both their number and repopulation potential. *J Exp Med* **191:** 253–264.

Dorsch M, Goff SP. 1996. Increased sensitivity to apoptotic stimuli in c-abl-deficient progenitor B-cell lines. *Proc Natl Acad Sci* **93:** 13131–13136.

Elhasid R, Sahar D, Merling A, Zivony Y, Rotem A, Ben-Arush M, Izraeli S, Bercovich D, Larisch S. 2004. Mitochondrial pro-apoptotic ARTS protein is lost in the majority of acute lymphoblastic leukemia patients. *Oncogene* **23:** 5468–5475.

Fesik SW. 2005. Promoting apoptosis as a strategy for cancer drug discovery. *Nat Rev Cancer* **5:** 876–885.

Gottfried Y, Rotem A, Lotan R, Steller H, Larisch S. 2004. The mitochondrial ARTS protein promotes apoptosis through targeting XIAP. *EMBO J* **23:** 1627–1635.

Hall PA, Russell SE. 2004. The pathobiology of the septin gene family. *J Pathol* **204:** 489–505.

Hall PA, Jung K, Hillan KJ, Russell SE. 2005. Expression profiling the human septin gene family. *J Pathol* **206:** 269–278.

Hanahan D, Weinberg RA. 2000. The hallmarks of cancer. *Cell* **100:** 57–70.

Harlin H, Reffrey SB, Duckett CS, Lindsten T, Thompson CB. 2001. Characterization of XIAP-deficient mice. *Mol Cell Biol* **21:** 3604–3608.

Harris AW, Pinkert CA, Crawford M, Langdon WY, Brinster RL, Adams J. 1988. The Eμ-myc transgenic mouse. A model for high-incidence spontaneous lymphoma and leukemia of early B cells. *J Exp Med* **167:** 353–371.

Ihara M, Kinoshita A, Yamada S, Tanaka H, Tanigaki A, Kitano A, Goto M, Okubo K, Nishiyama H, Ogawa O, et al. 2005. Cortical organization by the septin cytoskeleton is essential for structural and mechanical integrity of mammalian spermatozoa. *Dev Cell* **8:** 343–352.

Ihara M, Yamasaki N, Hagiwara A, Tanigaki A, Kitano A, Hikawa R, Tomimoto H, Noda M, Takanashi M, Mori H, et al. 2007. Sept4, a component of presynaptic scaffold and Lewy bodies, is required for the suppression of α-synuclein neurotoxicity. *Neuron* **53:** 519–533.

Iwasako K, Hatano E, Taura K, Nakajima A, Tada M, Seo S, Tamaki N, Sato F, Ikai I, Uemoto S, et al. 2008. Loss of Sept4 exacerbates liver fibrosis through the dysregulation of hepatic stellate cells. *J Hepatol* **49:** 768–778.

Jacobson MD, Weil M, Raff MC. 1997. Programmed cell death in animal development. *Cell* **88:** 347–354.

Jones JM, Datta P, Srinivasula SM, Ji W, Gupta S, Zhang Z, Davies E, Hajnoczky G, Saunders TL, Van Keuren ML, et al. 2003. Loss of Omi mitochondrial protease activity causes the neuromuscular disorder of mnd2 mutant mice. *Nature* **425:** 721–727.

Kim DS, Hubbard SL, Peraud A, Salhia B, Sakai K, Rutka JT. 2004. Analysis of mammalian septin expression in human malignant brain tumors. *Neoplasia* **6:** 168–178.

Kinoshita M. 2006. Diversity of septin scaffolds. *Curr Opin Cell Biol* **18:** 54–60.

Kissel H, Georgescu MM, Larisch S, Manova K, Hunnicutt GR, Steller H. 2005. The Sept4 Septin locus is required for sperm terminal differentiation in mice. *Dev Cell* **8:** 353–364.

Kondo M, Wagers AJ, Manz MG, Prohaska SS, Scherer DC, Beilhack GF, Shizuru JA, Weissman IL. 2003. Biology of hematopoietic stem cells and progenitors: Implications for clinical application. *Annu Rev Immunol* **21:** 759–806.

Kornbluth S, White K. 2005. Apoptosis in *Drosophila*: Neither fish nor fowl (nor man, nor worm). *J Cell Sci* **118:** 1779–1787.

Kremer BE, Adang LA, Macara IG. 2007. Septins regulate actin organization and cell-cycle arrest through nuclear accumulation of NCK mediated by SOCS7. *Cell* **130:** 837–850.

LaCasse EC, Mahoney DJ, Cheung HH, Plenchette S, Baird S, Korneluk RG. 2008. IAP-targeted therapies for cancer. *Oncogene* **27:** 6252–6275.

Larisch S, Yi Y, Lotan R, Kerner H, Eimerl S, Tony Parks W, Gottfried Y, Birkey Reffey S, de Caestecker MP, Danielpour D, et al. 2000. A novel mitochondrial septin-like protein, ARTS, mediates apoptosis dependent on its P-loop motif. *Nat Cell Biol* **2:** 915–921.

Liu Y, Elf SE, Miyata Y, Sashida G, Liu Y, Huang G, Di Giandomenico S, Lee JM, Deblasio A, Menendez S, et al. 2009. p53 regulates hematopoietic stem cell quiescence. *Cell Stem Cell* **4:** 37–48.

Longtine MS, DeMarini DJ, Valencik ML, Al-Awar OS, Fares H, De Virgilio C, Pringle JR. 1996. The septins: Roles in cytokinesis and other processes. *Curr Opin Cell Biol* **8:** 106–119.

Macara IG, Baldarelli R, Field CM, Glotzer M, Hayashi Y, Hsu SC, Kennedy MB, Kinoshita M, Longtine M, Low C, et al. 2002. Mammalian septins nomenclature. *Mol Biol Cell* **13:** 4111–4113.

Martins LM, Morrison A, Klupsch K, Fedele V, Moisoi N, Teismann P, Abuin A, Grau E, Geppert M, Livi GP, et al. 2004. Neuroprotective role of the Reaper-related serine protease HtrA2/Omi revealed by targeted deletion in mice. *Mol Cell Biol* **24:** 9848–9862.

Mehlen P, Puisieux A. 2006. Metastasis: A question of life or death. *Nat Rev Cancer* **6:** 449–458.

Meier P, Finch A, Evan G. 2000. Apoptosis in development. *Nature* **407:** 796–801.

Miller CL, Dykstra B, Eaves CJ. 2008. Characterization of mouse hematopoietic stem and progenitor cells. *Curr Protoc Immunol* **80:** 22B.2.1–22B.2.31. doi: 10.1002/0471142735.im22b02s80.

Morrison SJ, Wandycz AM, Akashi K, Globerson A, Weissman IL. 1996. The aging of hematopoietic stem cells. *Nat Med* **2:** 1011–1016.

Neufeld TP, Rubin GM. 1994. The *Drosophila* peanut gene is required for cytokinesis and encodes a protein similar to yeast putative budd neck filament proteins. *Cell* **77:** 371–379.

Nimer SD. 2008. MDS: A stem cell disorder—But what exactly is wrong with the primitive hematopoietic cells in this disease? *Hematology Am Soc Hematol Educ Program* **2008:** 43–51.

Oguro H, Iwama A. 2007. Life and death in hematopoietic stem cells. *Curr Opin Immunol* **19:** 503–509.

Okada H, Suh WK, Jin J, Woo M, Du C, Elia A, Duncan GS, Wakeham A, Itie A, Lowe SW, et al. 2002. Generation and characterization of Smac/DIABLO-deficient mice. *Mol Cell Biol* **22:** 3509–3517.

Passegue E, Jamieson CH, Ailles LE, Weissman IL. 2003. Normal and leukemic hematopoiesis: Are leukemias a stem cell disorder or a reacquisition of stem cell characteristics? *Proc Natl Acad Sci* **100:** 11842–11849.

Pelengaris S, Khan M, Evan G. 2002. c-MYC: More than just a matter of life and death. *Nat Rev Cancer* **2:** 764–776.

Reed JC. 2003. Apoptosis-targeted therapies for cancer. *Cancer Cell* **3:** 17–22.

Reed JC, Pellecchia M. 2005. Apoptosis-based therapies for hematologic malignancies. *Blood* **106:** 408–418.

Reya T, Morrison SJ, Clarke MF, Weissman IL. 2001. Stem cells, cancer and cancer stem cells. *Science* **414:** 105–109.

Rossi DJ, Jamieson CH, Weissman IL. 2008. Stems cells and the pathways to aging and cancer. *Cell* **132:** 681–696.

Salvesen GS, Duckett CS. 2002. IAP proteins: Blocking the road to death's door. *Nat Rev Mol Cell Biol* **3:** 401–410.

Santos J, Cerveira N, Bizarro S, Ribeiro FR, Correia C, Torres L, Lisboa S, Vieira J, Mariz JM, Norton L, et al. 2010. Expression pattern of the septin gene family in acute myeloid leukemias with and without MLL-SEPT fusion genes. *Leuk Res* **34:** 615–621.

Schile AJ, Garcia-Fernandez M, Steller H. 2008. Regulation of apoptosis by XIAP ubiquitin-ligase activity. *Genes Dev* **22:** 2256–2266.

Scott CL, Schuler M, Marsden VS, Egle A, Pellegrini M, Nesic D, Gerondakis S, Nutt SL, Green DR, Strasser A. 2004. Apaf-1 and caspase-9 do not act as tumor suppressors in myc-induced lymphomagenesis or mouse embryo fibroblast transformation. *J Cell Biol* **164:** 189–196.

Shi Y. 2004. Caspase activation, inhibition, and reactivation: A mechanistic view. *Protein Sci* **13:** 1979–1987.

Sidman CL, Shaffer DJ, Jacobsen K, Vargas SR, Osmond DG. 1993. Cell populations during tumorigenesis in Eμ-myc transgenic mice. *Leukemia* **7:** 887–895.

Spangrude GJ, Heimfeld S, Weissman IL. 1988. Purification and characterization of mouse hematopoietic stem cells. *Science* **241:** 58–62.

Spiliotis ET, Kinoshita M, Nelson WJ. 2005. A mitotic septin scaffold required for Mammalian chromosome congression and segregation. *Science* **307:** 1781–1785.

Steller H. 2008. Regulation of apoptosis in *Drosophila*. *Cell Death Differ* **15:** 1132–1138.

Strasser A, Harris AW, Bath ML, Cory S. 1990. Novel primitive lymphoid tumours induced in transgenic mice by cooperation between myc and bcl-2. *Nature* **348:** 331–333.

Szilvassy SJ, Cory S. 1993. Phenotypic and functional characterization of competitive long-term repopulating hematopoietic stem cells enriched from 5-fluorouracil-treated murine marrow. *Blood* **81:** 2310–2320.

Tan BT, Park CY, Ailles LE, Weissman IL. 2006. The cancer stem cell hypothesis: A work in progress. *Lab Invest* **86:** 1203–1207.

Thompson CB. 1995. Apoptosis in the pathogenesis and treatment of disease. *Science* **267:** 1456–1462.

Vaux DL, Silke J. 2005. IAPs, RINGs and ubiquitylation. *Nat Rev Mol Cell Biol* **6:** 287–297.

Vaux DL, Aguila HL, Weissman IL. 1992. Bcl-2 prevents death of factor-deprived cells but fails to prevent apoptosis in targets of cell mediated killing. *Int Immunol* **4:** 821–824.

Weirich CS, Erzberger JP, Barral Y. 2008. The septin family of GTPases: Architecture and dynamics. *Nat Rev Mol Cell Biol* **9:** 478–489.

White K, Grether ME, Abrams JM, Young L, Farrell K, Steller H. 1994. Genetic control of programmed cell death in *Drosophila*. *Science* **264:** 677–683.

Yang Y, Fang S, Jensen JP, Weissman AM, Ashwell JD. 2000. Ubiquitin protein ligase activity of IAPs and their degradation in proteasomes in response to apoptotic stimuli. *Science* **288:** 874–877.

Yilmaz OH, Valdez R, Theisen BK, Guo W, Ferguson DO, Wu H, Morrison SJ. 2006. Pten dependence distingues haematopoietic stem cells from leukaemia-initiating cells. *Nature* **441:** 475–482.